Design and Performance Analysis of G-Shaped Compact ACS Fed 4-Port MIMO Antenna for Triple Frequency Band Applications

Praveen V. Naidu[1, 2, *], Akkapanthula Saiharanadh[1, 2, 4], Dhanekula Maheshbabu[1, 2], Arvind Kumar[1, 3], and Neelima Vummadisetty[2]

Abstract—In this paper, a novel compact single element G-shaped Asymmetric Coplanar Strip (ACS) fed antenna and its four-element printed multiple-input multiple-output (MIMO) antenna have been presented with multi-band frequency characteristics. The proposed MIMO antenna has been fabricated on an FR-4 substrate $(46 \times 46 \times 1.6)\,\text{mm}^3$ with dielectric constant $\varepsilon_r = 4.4$. The desired isolation between the elements $(-18\,\text{dB})$ is achieved by placing the antenna elements orthogonal to each other. Simulated and measured results show that return loss (S_{11}) for the proposed MIMO antenna is less than $-10\,\text{dB}$ in the operating bands, with frequency ranging 2.30–2.45 GHz, 3.36–3.65 GHz, and 4.53–5.88 GHz, respectively, which ensures its operation in multiple frequency bands. Moreover, these bands are obtained for 2.3 GHz WiBro,LTE and 5G NR to cover B40/B42/N30/N40/N97 together with 3.5 GHz/5 GHz WiMAX/WLAN band applications. Meanwhile, the diversity performance characteristics like ECC (Envelope Correlation Coefficient), MEG (Mean Effective Gain), DG (Diversity Gain), Total Active Reflection Coefficient (TARC), and Channel Capacity Loss (CCL) have been calculated and are presented in this paper. The correlation coefficient is found to be less than 0.001 with a diversity gain greater than 9.95, and an acceptable channel capacity loss is less than 0.4 bits/s/Hz.

1. INTRODUCTION

Recently the fourth-generation wireless communication has relied on three major technologies, i.e., orthogonal frequency division multiple access (OFDMA), adaptive modulation and coding (AMC), and multiple input multiple output (MIMO) technology. The first two technologies describe how the data are coded and transmitted in wireless channels, and the third technology (MIMO) deals with the need of multiple antennas. However, data can be sent against multipath fading channel by using multiple antennas at transmitter and multiple antennas at receiving end. As the data have been sent with the aid of multiple antennas, we can expect a good replica at the receiver end. Most importantly data rate also increases which is a major advantage with using MIMO antenna technology. Furthermore, the design of MIMO antennas with compact size, wideband or multiband frequency operation, and good channel capacity that highly depends on mutual coupling (isolation) is a great challenging task for researchers and engineers. To address the above challenges, different types of techniques like using neutralization lines [1], EBG structures [2], metamaterial absorbers [3], and parasitic elements [4] play a key role in the enhancement of isolation between the radiators. The use of ACS feeding [5–7], compact antennas [8–10] plays a vital role in reducing the overall size of the system. The clever use of a simple geometry enables us to configure the radiating elements with maximum possible inter-element distance that results in good isolation. As a result, this ACS MIMO design system is relatively compact, simple, yet performs harmoniously with minimum of fabrication efforts. The following Table 1 gives a brief summary of published literature [11–26] and its summary.

* Corresponding author: Praveen Vummadisetty Naidu (praveennaidu468@gmail.com).
[1] Velagapudi Ramakrishna Siddhartha Engineering College, Vijayawada 520007, India. [2] Department of R&D, NPHSAT Systems Pvt Ltd, Vijayawada 520007, India. [3] University of East London, UK. [4] DRDO, Hyderabad, India.

Table 1. Comparison of various existing antenna performances with proposed design.

Ref. No	Size (mm × mm)	Area (mm²)	Ports	Operating Bands (GHz)	Minimum isolation	Avg Gain	ECC	CCL
11.	65.3 ∗ 65.3	4264.09	2	2.4/3.5	−12.4	2.6 dB	< 0.01	-
12.	50 ∗ 50	2500	2	2.4/3.5/5.5	−18	3.3 dB	< 0.03	-
13.	75 ∗ 66	4950	2	2.4/5.5	−22	3.34 dB	< 0.25	-
14.	100 ∗ 55	5500	2	2.45/5.25	−25	-	0.001	-
15.	60 ∗ 100	6000	2	2.45/5.5	−16	-0.825 dBi	< 0.1	-
16.	60 ∗ 130	7800	4	2.45/5.2/5.8	< −15	3 dB	< 0.25	-
17.	60 ∗ 60	3600	4	2.5/5.2	−18	3.82 dB	< 0.004	-
18.	90 ∗ 40	3600	2	3.3	−17	1.2 dBi	0.005	0.4
19.	54.7 ∗ 37.5	2051.25	4	5.2	−44	-	-	-
20.	50 ∗ 80	4000	2	2.4/5.8	−20	4.12 dB	0.01	-
21.	30 ∗ 65	1950	2	2.4/5.5	−25	4.34 dB	< 0.1	-
22.	60 ∗ 60	3600	2	2.44/5.48	−25	-	< 0.08	-
23.	55 ∗ 64	3520	2	2.35/3.5	−15	2.76 dB	< 0.001	-
24.	100 ∗ 130	13000	2	2.44/5.5	−22	2.1 dB	0.12	-
25.	84 ∗ 26	2184	4	3.5/5.5/7	−28	-	-	-
26.	58 × 55	3132	2	2.1/2.5/3.5/5.2/5.8	< −14	2.5 dB	< 0.02	-
Proposed	**46 ∗ 46**	**2116**	**4**	**2.3/3.5/5.2/5.5/5.8**	**−18**	**4 dB**	**< 0.001**	**< 0.4**

In this research article, an ACS-fed G-shaped 4-port MIMO antenna with tri-band characteristics has been designed and developed. The diversity performance metrics like ECC, DG, TARC, MEG, and CCL have been calculated and given in the following sections.

2. ANTENNA SINGLE ELEMENT DESIGN AND RESULTS

The geometrical structure of compact G shape monopole antenna is shown in Fig. 1(a). The proposed unique structure is realized on a cost effective FR-4 substrate (in Fig. 1(b)). The lateral ground plane with square shape is designed with dimensions $4 \times 4 \, \text{mm}^2$, and the overall dimensions of proposed antenna are $11.2 \times 22.2 \times 1.6 \, \text{mm}^3$. A standard SMA connector is used for terminating 50 ohm ACS fed line with signal strip of length 3 mm with a minimum gap of 0.5 mm maintained between the feed line and partial ground plane. By varying the parameters of three radiators and feeding structure, a good impedance matching is observed in design. The parameters for proposed design shown in Fig. 1(a) are as follows: $W = 11.2$, $L = 22.2$, $L1 = 5$, $L2 = 1.3$, $L3 = 1.8$, $L4 = 1.2$, $L5 = 1.3$, $L6 = 2.4$, $L7 = 1.1$, $L8 = 1.9$, $L9 = 1$, $L10 = 3$, $L11 = 4$, $W1 = 4$, $W2 = 3$, $W3 = 4.1$, $W4 = 1.6$, $W5 = 3.2$, $W6 = 2.1$, $W7 = 2.6$, $W8 = 4.1$, $a = 0.9$, $b = 0.8$, $c = 0.3$, $E = 0.2$, $k = 0.7$, $F1$, $g1 = 1.7$, $g2 = 1.2$, $G = 0.5$ (all values are in mm).

The operational frequency (f_r) for the proposed antenna is derived from Equations (1) and (2), and the equations for proper impedance matching are given in Equations (3) and (4). The CST MWS (2018) which operates based on finite integration method is used for the design of proposed antenna achieving a tri-band operation. The evolution of each radiator and its $|S_{11}|$ characteristics for 3 radiating modes are shown in Figs. 2(a) & (b). The first resonant mode is obtained by Antenna 1 in Fig. 2(a) which is a simple monopole radiator and indicated with dashed brown colour line. In addition to Antenna 1, a rectangular strip is introduced as shown in Antenna 2, which helps in obtaining dual frequencies of operation at 3.5/5.2 GHz which are indicated by green dashed and dotted line. Finally, a novel G
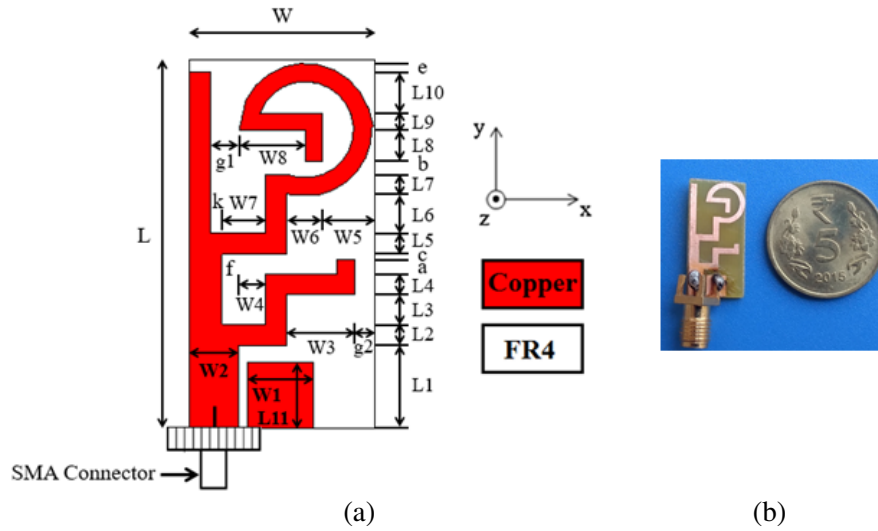
Figure 1. (a) Geometry of proposed G shape unit element. (b) Single element prototype of proposed G shape unit element.
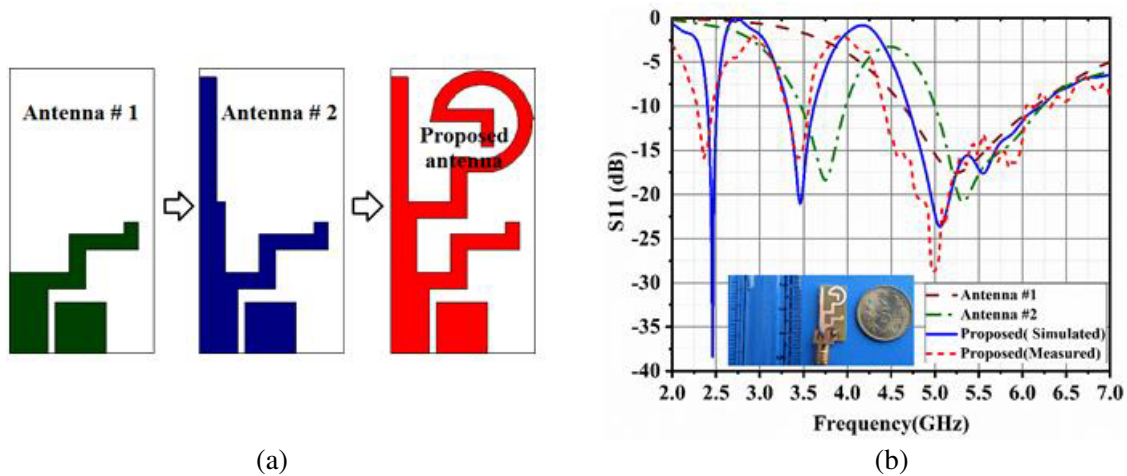

Figure 2. (a) Evolution of unit element. (b) Return loss characteristics during evolution and its measured result.

shape radiator is introduced which additionally operates at 2.4 GHz. The proposed antenna resonates at 2.3/3.5/5 GHz frequencies covering WiBro, LTE, and 5G NR to cover B40/B42/N30/N40/N97 together with 3.5 GHz/5 GHz WiMAX/WLAN band applications. The surface current distributions with evolution and at resonant frequencies can be observed from Fig. 3.

A parametric study (in Fig. 4) is carried out while the proposed G shape unit element is designed. When parameter 'a' (in Fig. 4(a)) is increased to 1.2 mm, the resonant frequency will be at 5 GHz. With further increasing 'a' to 1.5 mm, the higher band shifts towards left, and the resonant frequency changes. At $a = 0.9$ mm, the antenna resonates at 5.2 GHz which is more suitable for WLAN applications. When $x1$ (in Fig. 4(b)) is decreased to 0.9 mm, the resonant frequency will be at 2.5 GHz. Further, if we increase $x1$ to 1.4 mm which results in electrical length getting increased, and the frequency band shifts towards lower side. With further increasing $x1$ to 1.9 mm, the antenna covers both WiBro and partial Bluetooth applications and resonates at 2.4 GHz. Furthermore, $y1$ (in Fig. 4(c)) plays a key role in antenna which will have impact on middle band for resonant frequency at 3.5 GHz. By varying $Y1$ from 8.8 mm to 9.8 mm, we can observe the shift in the middle band as $Y1$ increases, and the band shifts
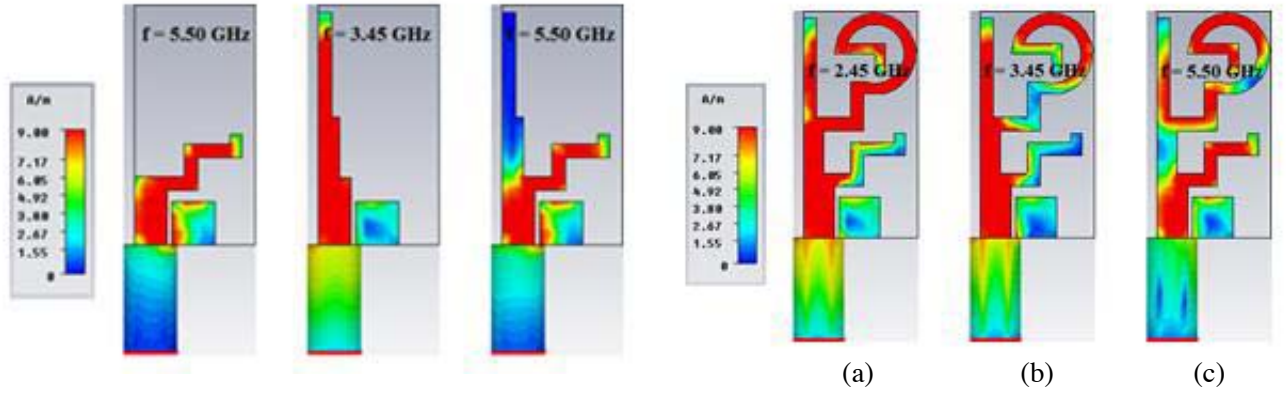
Figure 3. Surface current distribution of unit evolution element at (a) 2.45 GHz, (b) 3.45 GHz and (c) 5.5 GHz.

towards left; at $Y1 = 9.8$ mm, the antenna resonates at 3.5 GHz and is useful for WiMAX applications.

$$f_r = c/\left(\lambda_g\sqrt{\varepsilon_{eff}}\right) \tag{1}$$

$$\varepsilon_{eff} = \frac{\varepsilon_r + 1}{2} \tag{2}$$

$$Z_0 = \frac{60\prod K(k)}{\sqrt{\varepsilon_{eff}}K(k')} \tag{3}$$

where $k = a/b$, $k' = k' = \sqrt{1 - k^2}$ and $\frac{K(k)}{K(k')}$ is referred to the elliptical integral form acknowledged by

$$\frac{K(k)}{K(k')} = \begin{cases} \frac{\pi}{\ln\frac{2\left(1+\sqrt{k'}\right)}{\left(1-\sqrt{k'}\right)}} & 0 \le k \le \frac{1}{\sqrt{2}} \\ \frac{1}{\pi\ln\frac{2\left(1+\sqrt{k}\right)}{\left(1-\sqrt{k}\right)}} & \frac{1}{\sqrt{2}} \le k \le 1 \end{cases} \tag{4}$$

3. FOUR-ELEMENT MIMO ANTENNA DESIGN

An anti-parallel configuration of unit element has been considered as the first choice in the process of designing G shape compact MIMO antenna. Next, the overall dimensions taken in this case are $23 \times 50 \times 1.6$ mm^3. However, in general if any two elements having radiating nature are placed closely, there is a chance of induced EMF at each other's ports, due to which there exists a strong mutual coupling between them. Since there is no physical connection between ground planes, the existence of mutual coupling can be attributed to the far field coupling. Also due to the symmetric nature of radiation pattern at lower operating band, there will be no use of this anti-parallel configuration. Moreover, Inter-element spacing between the two elements in this configuration is equal to 28 mm. As a result, the existence of strong coupling with the help of surface current distribution is illustrated in Fig. 5(a). It can be realized that some amount of current is coupled into the second element. Further, to avoid the coupling of the far fields, the orthogonal placement of antenna is the best choice. It is clearly seen from Fig. 5(b) that both the ports are sufficiently isolated from each other, and a very small amount of current is coupled into the second radiator. The overall dimensions in this case are $23 \times 46 \times 1.6$ mm^3 with an inter element spacing equal to 12 mm. However, the drawback of this configuration, despite of having the highest amount of isolation there, will be a displacement of lower operating bands causing non-concurrent return loss characteristics. In order to overcome these drawbacks of anti-parallel and orthogonal configurations, a four-port orthogonal configuration as shown in Fig. 5(c) is considered. Here, the required isolation between ports is achieved by maintaining a sufficient spacing of 17.3 mm

between the unit elements. It is ascertained from Fig. 5(c) that there is only a minimum amount of mutual coupling between the diagonal elements of the proposed MIMO antenna array.

To ensure the MIMO operation without any performance degradation, it is required to have mutual coupling less than -15 dB. Fig. 6 shows the mutual coupling between ports 1 & 2 in various configurations.
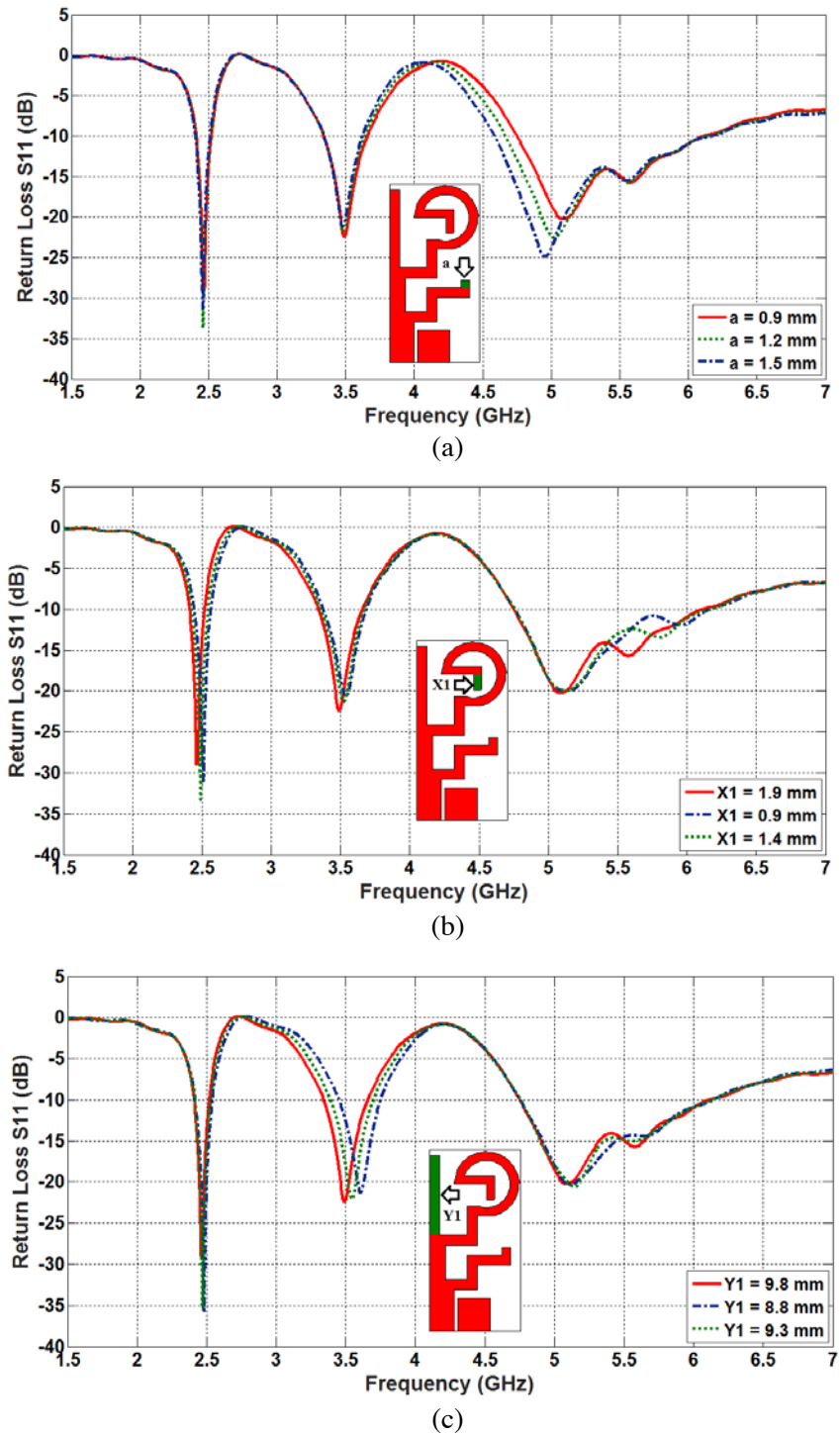

(a)

(b)

(c)

Figure 4. $|S_{11}|$ characteristics of proposed antenna parameters 'a', '$X1$', and '$Y1$', for various lengths.

(a)   (b)

(c)
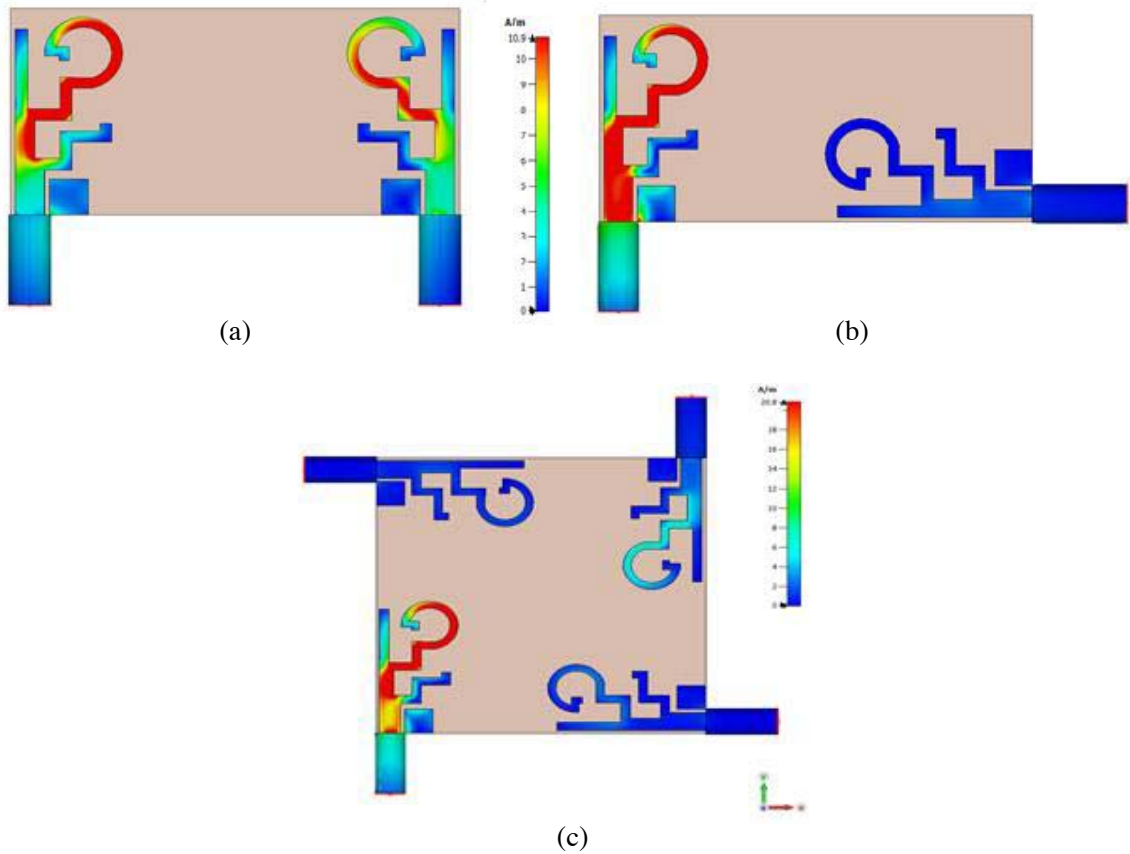
Figure 5. Surface current distribution for (a) anti-parallel configuration, (b) orthogonal, configuration and (c) proposed MIMO configuration at 2.3 GHz.
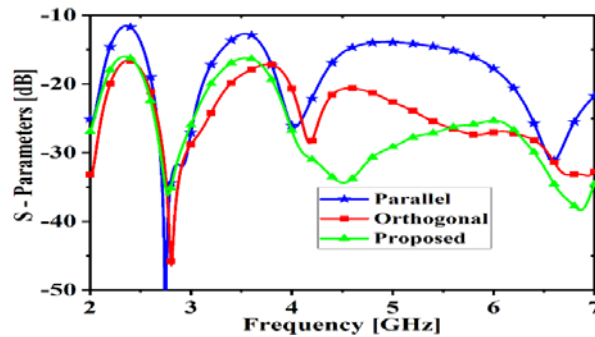

Figure 6. Study of isolation between port-1 and port-2 in different configurations.

The proposed compact four-port ACS fed G-shaped MIMO antenna has been designed using an FR4 substrate having dimensions of $46 \times 46 \times 1.6 \, \text{mm}^3$. In the meantime, a square-shaped geometry is chosen for the placement of antenna elements to achieve the shift in the individual resonances of elements as occurred in the case of two-port orthogonal configuration. Furthermore, pattern diversity is achieved through this orthogonal placement which helps in maintaining minimal mutual coupling between closely spaced antenna elements. The effective electrical length of the individual radiating paths is increased as the elements are placed close to each other, due to which there is a significant amount of frequency shift in the lower and middle operating bands. So, optimization of the path lengths needs to be done to tune the MIMO antenna array to desired operating bands. This is the only phenomenon behind the
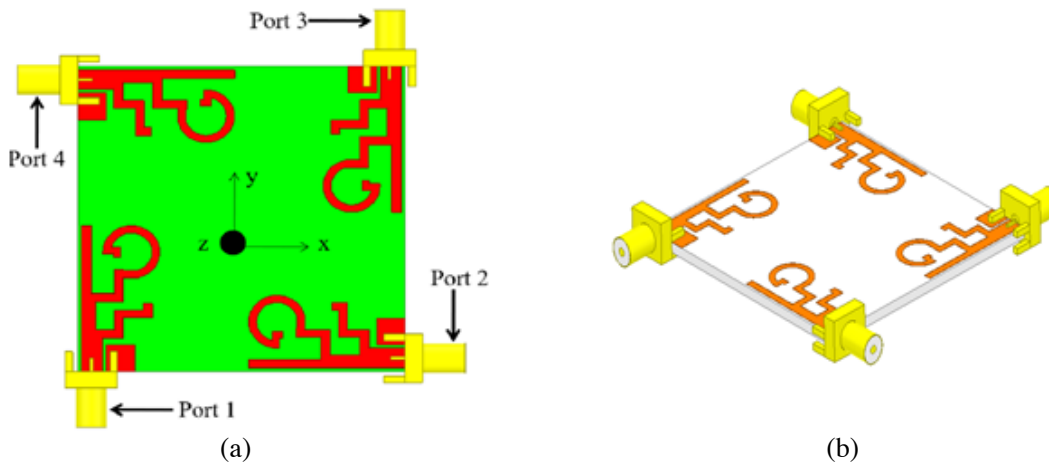
(a)   (b)

Figure 7. (a) Geometry of the proposed four-port ACS fed G shape MIMO antenna design. All dimension are in mm. (b) Isometric view of proposed four port G shape MIMO antenna.

difference between the geometries of unit element and MIMO array antenna elements, and the geometry of proposed G shape MIMO antenna is shown in Figs. 7(a) & (b).

4. FOUR ELEMENT MIMO ANTENNA RESULTS

For the validation of simulated results, a prototype has been fabricated on an FR-4 substrate and tested with the help of Keysight fieldfox microwave Analyzer N9918A as shown in Fig. 8. Moreover, the simulated and measured values of $|S_{11}|$, $|S_{12}|$, and $|S_{13}|$ are plotted in Fig. 9. For the simulation purpose of proposed antenna, the electromagnetic simulation tool CST Microwave studio has been used. As we can observe, the impedance bandwidth of antenna in operating band from 2.3 GHz to 2.45 GHz, which corresponds to 150 MHz, covers WiBro applications, LTE and 5G NR to cover **B40/B42/N30/N40/N97** frequency bands, the second frequency band operating from 3.36 GHz to 3.65 GHz with a bandwidth of 290 MHz having center frequency at 3.5 GHz useful for WiMAX applications, and finally higher band from 4.53 GHz to 5.88 GHz with a bandwidth 135 MHz covering WLAN applications. Apart from this, the simulated and measured isolations between the radiators S_{12} and S_{13} have been calculated and are found to be -18 dB which can be seen from Fig. 9. On the other hand, it is determined the efficiency and gain are important parameters in determining antenna

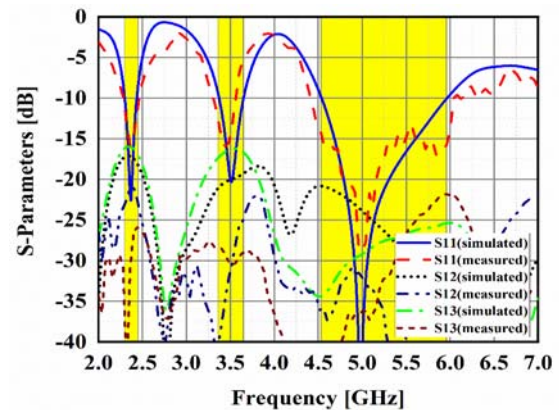**Figure 8.** Testing of prototype using Keysight fieldfox microwave Analyzer N9918A.

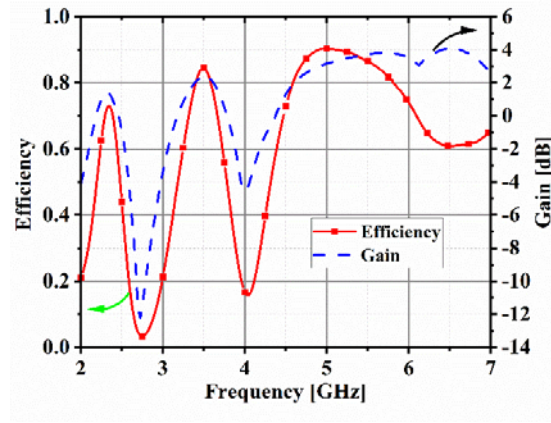**Figure 9.** Simulated and measured S-parameters of the proposed G shaped MIMO antenna.

Figure 10. Measured radiation efficiency and gain of proposed G-shape ACS fed MIMO antenna.

performance. Consequently, the proposed 4-element G-shape ACS fed MIMO array operates with a measured peak gain of 4 dB having efficiency 75–85% (in Fig. 10). In the meantime, the measured radiation patterns for the proposed electrically small G-shape MIMO antenna in both E-plane and H-plane at various frequencies are given in Fig. 11.

5. MIMO ANTENNA DIVERSITY PERFORMANCE ANALYSIS [27–29]

In this section, the figure of metrics for the multi-input multi-output antenna system has been evaluated. This helps to comprehend the performance of the proposed antenna. The following parameters [27–29] such as ECC (Envelope Correlation Coefficient), MEG (Mean Effective Gain), DG (Diversity Gain), Total Active Reflection Coefficient (TARC), and Channel Capacity Loss (CCL) are calculated (simulated and measured) and presented in this section.

5.1. ECC and DG

Facing complexity in 3D far filed measurement and calculation, correlation coefficient is calculated with the help of S-parameters. As per [18], the envelope correlation coefficient can be calculated with the help of S-parameters using Equation (5). Fig. 12(a) shows the envelope correlation coefficient across the operating bands. Both simulated and measured ECCs are less than 0.001 in the operating bands.

$$\rho_e = \left| \frac{\left| S_{ii}^* S_{ij} + S_{ji}^* S_{jj} \right|}{\left| \left(1 - |S_{ii}|^2 - |S_{ij}|^2 \right) \left(1 - |S_{jj}|^2 - |S_{ji}|^2 \right) \right|^{\frac{1}{2}}} \right|^2 \tag{5}$$

Diversity gain (DG) can be used to describe the gain enhancement of a MIMO-antenna system in a combined signal over time-averaged SNR. DG can be evaluated using Equation (6) and achieve greater than 9.95 in operating band, which can be seen from Fig. 12(b)

$$\mathrm{DG} = \sqrt{\left(1 - |0.99\rho_e|^2 \right)} \tag{6}$$

5.2. Mean Effective Gain (MEG)

Mean Effective Gain is the amount of power received by antenna elements in a MIMO antenna compared to isotropic antenna in a fading environment. It is one of the important measures in defining MIMO antenna performance. The Mean Effective Gain can be calculated with the help of S-parameters using Equations (7)–(12). The difference between any two MEGs must be < 3 dB and achieved for the

proposed MIMO antenna which is shown in Fig. 13.

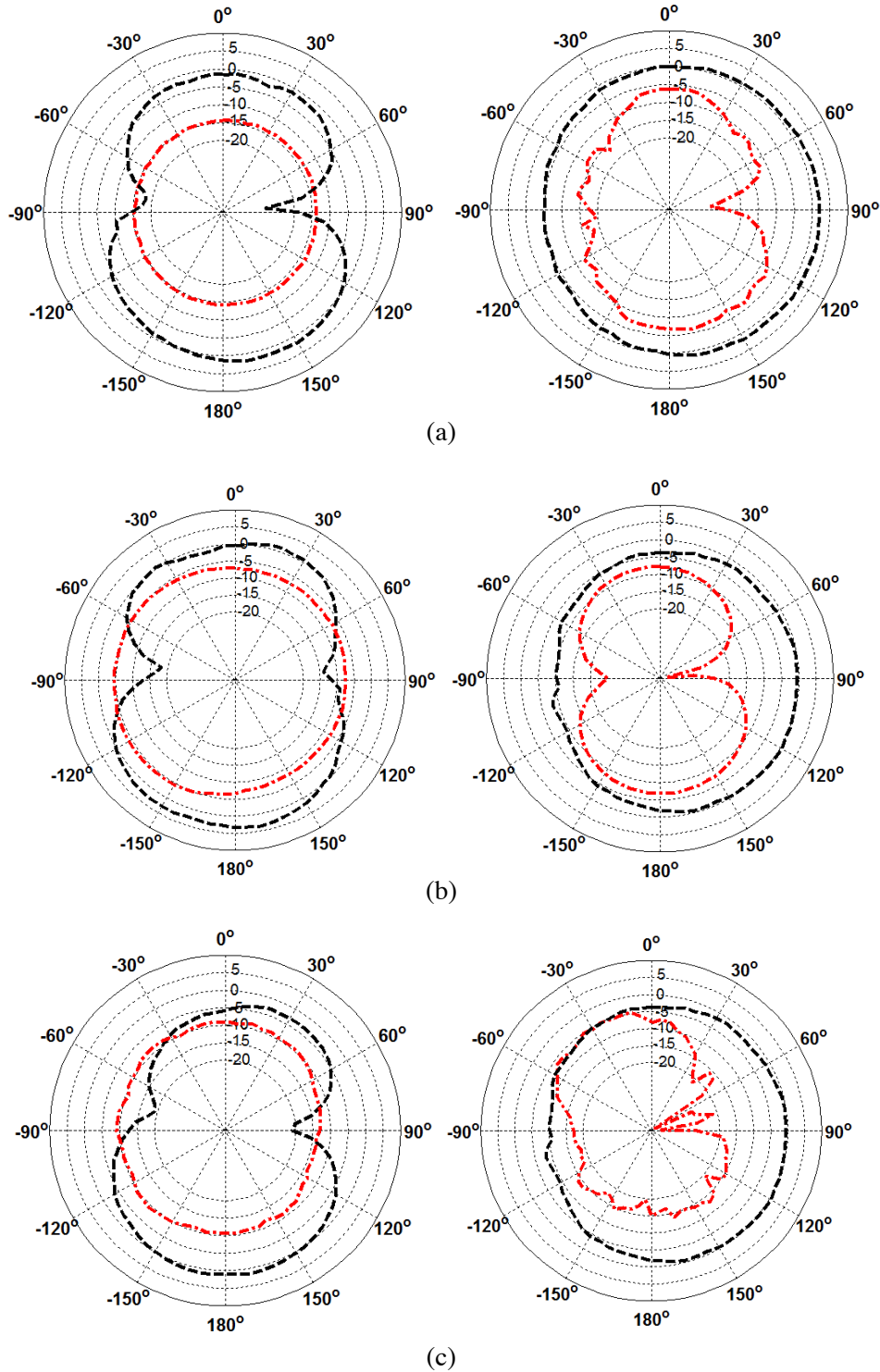$$\text{MEG} = 0.5 \left[1 - \sum_{j=1}^{N} |S_{ij}|^2 \right] \tag{7}$$

Figure 11. Normalized radiation patters for proposed G shape MIMO antenna at various frequencies (a) E & H plane at 2.4 GHz, (b) E & H plane at 3.5 GHz, (c) E & H plane at 5.5 GHz.
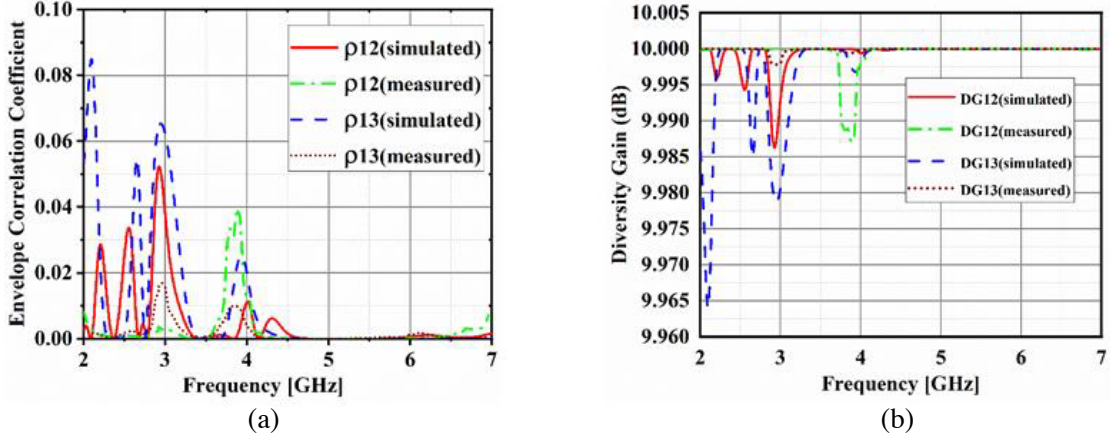
Figure 12. (a) Envelope Correlation Coefficient (ECC). (b) Diversity Gain (DG) of the proposed G-shaped MIMO ACS fed triple band antenna.

also

$$|\text{MEG}_i - \text{MEG}_j| < 3\,\text{dB} \tag{8}$$

So, MEG can be written as

$$\text{MEG1} = 0.5\left[1 - |S_{11}|^2 - |S_{12}|^2 - |S_{13}|^2 - |S_{14}|^2\right] \tag{9}$$

$$\text{MEG2} = 0.5\left[1 - |S_{21}|^2 - |S_{22}|^2 - |S_{23}|^2 - |S_{24}|^2\right] \tag{10}$$

$$\text{MEG3} = 0.5\left[1 - |S_{31}|^2 - |S_{32}|^2 - |S_{33}|^2 - |S_{34}|^2\right] \tag{11}$$

$$\text{MEG4} = 0.5\left[1 - |S_{41}|^2 - |S_{42}|^2 - |S_{43}|^2 - |S_{44}|^2\right] \tag{12}$$

Figure 13(b) shows the comparison of simulated & measured ECCs & MEG values calculated as per the equations provided in [28–30] based on far fields model. Solid lines indicate the simulated values whereas dotted lines with legends being suffixed with '*m*' indicate the measured values of the respective parameters. An analytical comparison between values of ECCs obtained in simulated and measured quantities shows a very little amount of deviation in operating bands that have radiating
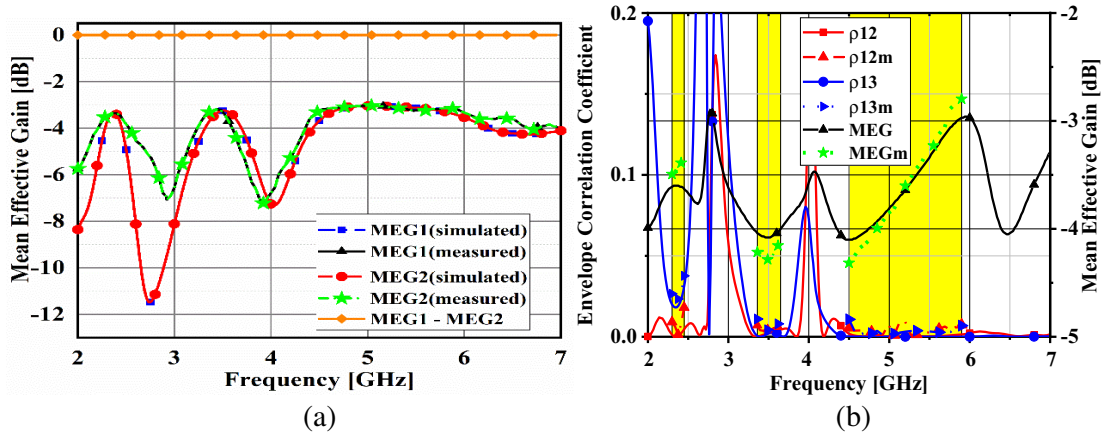

Figure 13. (a) Mean Effective Gain (MEG) of the proposed G shaped MIMO antenna. (b) Comparison of simulated & measured ECC & MEG values of proposed MIMO antenna calculated from far fields.

efficiencies more than 90%. A very low value of ECC in upper band can be attributed to the fact that interelement spacing is more than half a wavelength which is a criterion to achieve satisfactory MIMO performance. $\rho 12$ is very low in magnitude due to the orthogonal field interaction between the respective elements. Due to symmetry in presented design, the radiation patterns of elements of array antenna remain identical, and therefore only a single curve of MEG is shown in Fig. 13(b). MEG is calculated assuming Gaussian distribution of power densities with cross polarization ratio being 6 dB (Indoor communications).

5.3. TARC

S-parameters and Total Active Reflection Coefficient can only characterize single element antenna system. Hence, TARC is used to realize the original behaviour of S-parameters for different phase angles. Subsequently, the comparison of different excitation angels at the ports is given in Fig. 14 and calculated using Equation (13).

$$\text{TARC} = \frac{\sqrt{\sum_{i=1}^{N} \left| S_{i1} + \sum_{m=2}^{N} S_{im} e^{j\theta_{m-1}} \right|^2}}{\sqrt{N}} \tag{13}$$
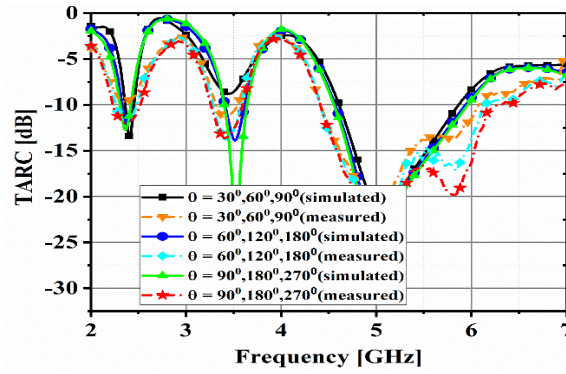

Figure 14. The Total Active Reflection Coefficient (TARC) of the proposed radiating structure versus frequency.

5.4. Channel Capacity Loss (CCL)

As the number of MIMO antenna elements increases, the channel capacity experiences a divergence from theoretical prediction of linear relation of increase in channel capacity with increase in antenna elements. However, this divergence causes a loss, is measured by CCL [18] and calculated by following Equations (14)–(16). The simulated and measured results of CCL and Channel Capacity can be seen from Fig. 15(a). The acceptable limit of CCL is 0.4 bits/s/Hz, and for the proposed MIMO antenna CCL is less than 0.4 bits/s/Hz, shown in Fig. 15(a), and Fig. 15(b) represents channel capacity.

$$C_{\text{loss}} = -\log_2 \det(\alpha^R) \tag{14}$$

$$\alpha^R = \begin{bmatrix} \alpha_{11} & \alpha_{12} & \alpha_{13} & \alpha_{14} \\ \alpha_{21} & \alpha_{22} & \alpha_{23} & \alpha_{24} \\ \alpha_{31} & \alpha_{32} & \alpha_{33} & \alpha_{34} \\ \alpha_{41} & \alpha_{42} & \alpha_{43} & \alpha_{44} \end{bmatrix}$$

$$\alpha_{ii} = 1 - \left(\sum_{j=1}^{N} |S_{ij}|^2 \right) \tag{15}$$

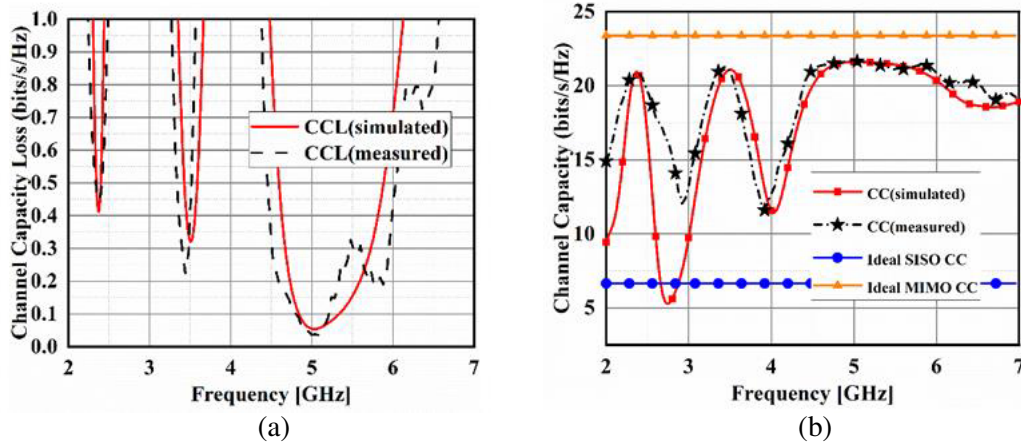$$\alpha_{ij} = -\left(S_{ii}^* S_{ij} + S_{ji}^* S_{jj} \right) \tag{16}$$

Figure 15. (a) The Channel Capacity Loss in bits/s/Hz. (b) Channel Capacity in bits/s/Hz of the proposed G shape MIMO antenna.

Channel capacity is calculated using equations presented in [28, 29], and a maximum capacity achieved using the proposed radiating array is 21.65 bits/s/Hz while an ideal four-element array achieves a typical capacity of 23.68 bits/s/Hz.

6. CONCLUSION

In this paper, a 4-port tri-band G-shaped MIMO ACS fed antenna for 2.3 GHz WiBro, LTE, and 5G NR to cover B40/B42/N30/N40/N97 and 5 GHz Wi-MAX/WLAN applications has been proposed and realized on an FR-4 substrate of thickness 1.6 mm with an overall area of 46×46 mm^2. The proposed antenna operates in triple frequency bands ranging 2.3–2.45 GHz, 3.36–3.65 GHz, and 4.53–5.88 GHz, respectively, with desired radiation patterns and an average peak gain of 4 dB. In addition, the proposed antenna has mutual coupling less than -18 dB which is achieved by placing elements orthogonal to each other. The ECC of proposed MIMO antenna is found to be less than 0.001 with a diversity gain greater than 9.95 dB in the operating bands. At this time, the CCL value is found to be less than 0.3 bits/s/Hz in two higher operating bands and 0.4 bits/s/Hz in lower band. Following the diversity performance characteristics like ECC, MEG, DG, CCL and TARC are calculated and are in acceptable limits which confirms that the proposed design is suitable for MIMO applications.

ACKNOWLEDGMENT

REFERENCES

1. Kayabasi, A., A. Toktas, E. Yigit, and K. Sabanci, "Triangular quad-port multi-polarized UWB MIMO antenna with enhanced isolation using neutralization ring," *AEU-International Journal of Electronics and Communications*, Vol. 85, 47–53, 2018.

2. Naser-Moghadasi, M., R. Ahmadian, Z. Mansouri, F. B. Zarrabi, and M. Rahimi, "Compact EBG structures for reduction of mutual coupling in patch antenna MIMO arrays," *Progress In Electromagnetics Research C*, Vol. 53, 145–154, 2014.

3. Garg, P. and P. Jain, "Isolation improvement of MIMO antenna using a novel flower shaped metamaterial absorber at 5.5 GHz WiMAX band," *IEEE Transactions on Circuits and Systems II: Express Briefs*, Vol. 67, No. 4, 675–679, 2019.

4. Khan, M. S., A. D. Capobianco, M. F. Shafique, B. Ijaz, A. Naqvi, and B. D. Braaten, "Isolation enhancement of a wideband MIMO antenna using floating parasitic elements," *Microwave and Optical Technology Letters*, Vol. 57, No. 7, 1677–1682, 2015.

5. Kumar, A. and P. V. Naidu, "A novel compact printed ACS fed dual-band antenna for Bluetooth/WLAN/WiMAX applications," *2016 Progress In Electromagnetic Research Symposium (PIERS)*, 2000–2003, Shanghai, China, Aug. 8–11, 2016.

6. Raj, R. K., M. Joseph, M. N. Suma, and P. Mohanan, "Compact asymmetric coplanar strip fed monopole antenna for multiband applications," *IEEE Transactions on Antennas and Propagation*, Vol. 55, No. 5, 2351–2357, 2007.

7. Kuma, A., et al., "A compact uniplanar ACS fed multi band low cost printed antenna for modern 2.4/3.5/5 GHz applications," *Microsystem Technologies*, Vol. 24, No. 3, 1413–1422, 2018.

8. Kuma, R., et al., "Simulation, design of compact multi-band microstrip slot antennas for WiMAX/WLAN and UWB applications," *Wireless Personal Communication*, Vol. 80, No. 3, 1175–1192, 2015.

9. Naid, P. and R. Kumar, "Design of CPW-fed dual-band printed monopole antennas for LTE/WiMAX/WLAN and UWB applications," *Progress In Electromagnetics Research C*, Vol. 54, 103–116, 2014.

10. Vummadisetty, P. N., et al., "Design of compact octagonal slotted hexagonal and rectangular shaped monopole antennas for dual/UWB application," *Turkish Journal of Electrical Engineering & Computer Sciences*, Vol. 24, No. 4, 2806–2824, 2016.

11. Malviya, L., M. V. Kartikeyan, and R. K. Panigrahi, "Offset planar MIMO antenna for omnidirectional radiation patterns," *International Journal of RF and Microwave Computer-Aided Engineering*, Vol. 28, No. 6, e21274, 2018.

12. Fang, Q., D. Mi, and Y.-Z. Yin, "A tri-band MIMO antenna for WLAN/WiMAX application," *Progress In Electromagnetics Research Letters*, Vol. 55, 75–80, 2015.

13. Fang, H. S., C. Y. Wu, J. S. Sun, and J. T. Huang, "Design of a compact MIMO antenna with pattern diversity for WLAN application," *Microwave and Optical Technology Letters*, Vol. 59, No. 7, 1692–1697, 2017.

14. Zou, X., G. Wang, Y. Wang, and B. Zong, "Decoupling of dual-band closely spaced MIMO antennas based on novel coupled resonator structure," *Frequenz*, Vol. 72, Nos. 9–10, 437–441, 2018.

15. Lee, W. W. and Y. S. Cho, "A high-isolation MIMO antenna with dual-feed structure for WiFi of mobile phones," *Microwave and Optical Technology Letters*, Vol. 59, No. 4, 930–934, 2017.

16. Huang, H., Y. Liu, and S. X. Gong, "Four antenna MIMO system with compact radiator for mobile terminals," *Microwave and Optical Technology Letters*, Vol. 57, No. 6, 1281–1286, 2015.

17. Khan, M. U. and M. S. Sharawi, "A dual-band microstrip annular slot-based mimo antenna system," *Microwave and Optical Technology Letters*, Vol. 57, No. 2, 360–364, 2015.

18. See, C. H., R. A. Abd-Alhameed, Z. Z. Abidin, N. J. McEwan, and P. S. Excell, "Wideband printed MIMO/diversity monopole antenna for WiFi/WiMAX applications," *IEEE Transactions on Antennas and Propagation*, Vol. 60, No. 4, 2028–2035, 2012.

19. Ghosh, C. K., "A compact 4-channel microstrip MIMO antenna with reduced mutual coupling," *AEU-International Journal of Electronics and Communications*, Vol. 70, No. 7, 873–879, 2016.

20. Ling, X. and R. Li, "A novel dual-band MIMO antenna array with low mutual coupling for portable wireless devices," *IEEE Antennas and Wireless Propagation Letters*, Vol. 10, 1039–1042, 2011.

21. Cui, S., Y. Liu, W. Jiang, and S. X. Gong, "Compact dual-band monopole antennas with high port isolation," *Electronics Letters*, Vol. 47, No. 10, 579–580, 2011.

22. Deng, J. Y., Z. J. Wang, J. Y. Li, and L. X. Guo, "A dual-band MIMO antenna decoupled by a meandering line resonator for WLAN applications," *Microwave and Optical Technology Letters*, Vol. 60, No. 3, 759–765, 2018.

23. Sun, D., P. Wang, P. Gao, and Y. Zhang, "A novel dual-band MIMO antenna with two rings for WIMAX applications," *Journal of Electromagnetic Waves and Applications*, Vol. 32, No. 3, 274–280, 2018.

24. Addaci, R., A. Diallo, C. Luxey, P. Le Thuc, and R. Staraj, "Dual-band WLAN diversity antenna system with high port-to-port isolation," *IEEE Antennas and Wireless Propagation Letters*, Vol. 11, 244–247, 2012.

25. Liu, Y., M. Liu, F. Xu, J. Xu, and X. Huang, "A novel four-port high isolation MIMO antenna design for high-capacity wireless applications," *Microwave and Optical Technology Letters*, Vol. 60, No. 6, 1476–1481, 2018.

26. Mohammad-Ali-Nezhad, S. and H. R. Hassani, "A penta-band printed monopole antenna for MIMO applications," *Progress In Electromagnetics Research*, Vol. 84, 241–254, 2018.

27. Simons, R. N., *Coplanar Waveguide Circuits, Components, and Systems*, Wiley, Hoboken, 2004.

28. Sharawi, M. S., *Printed MIMO Antenna Engineering*, Artech House, 2004.

29. Biglieri, E., C. Robert, C. Anthony, et al., *MIMO Wireless Communications*, Cambridge University Press, 2007.

30. Honma, N. and K. Murata, "Correlation in MIMO antennas," *MDPI Electronics*, Vol. 9, 651, 2020, doi:10.3390/electronics9040651.